Conf-950472--6
SAND95-0721C

Scannerless range imaging with a square wave

Maritza R. Muguira, John T. Sackos, and Bart D. Bradley

Sandia National Laboratories
Electronic Fuzing and Sensors Department
PO Box 5800
Albuquerque, NM 87185-0859

ABSTRACT

Scannerless range imaging (SRI) is a unique approach to three dimensional imaging without scanners. SRI does, however, allow a more powerful light source to be used as compared to conventional Laser Radar (LADAR) systems due to the speed of operation associated with this staring system. As a result, a more efficient method of operation was investigated. As originally conceived, SRI transmits a continuous intensity modulated sinusoidal signal; however, a square wave driver is more energy efficient than a sinusoidal driver. In order to take advantage of this efficiency, a square wave operational methodology was investigated. As a result, four image frames are required for the extraction of range using a square wave to unambiguously resolve all time delays within one time period compared to a minimum of three frames for the sinusoidal wave.

1. SRI THEORY OF OPERATION

The SRI sensor invented and patented by Marion W. Scott in 1990 produces pixel registered range and reflectance images of all objects within a viewed scene. The theory of operation is summarized as follows: A light source is operated continuously and modulated sinusoidally to flood illuminate a target scene. A receiver which simultaneously views the illuminated scene imposes another periodic modulation on the receiver optical signal that is reflected back from the scene. The reflected optical signal exhibits a phase delay proportional to the distance traveled to and from the detected object in the scene. Spatially discreet demodulation is accomplished simultaneously for the entire image by mixing the return signal with a sinusoidally modulated gain in the receiver's image intensifier microchannel plate (MCP). The return signal is then detected by an integrating CCD array. At this point, each pixel in the digitized image contains both intensity and phase information. Figure 1 illustrates the schematic configuration of the SRI[1].

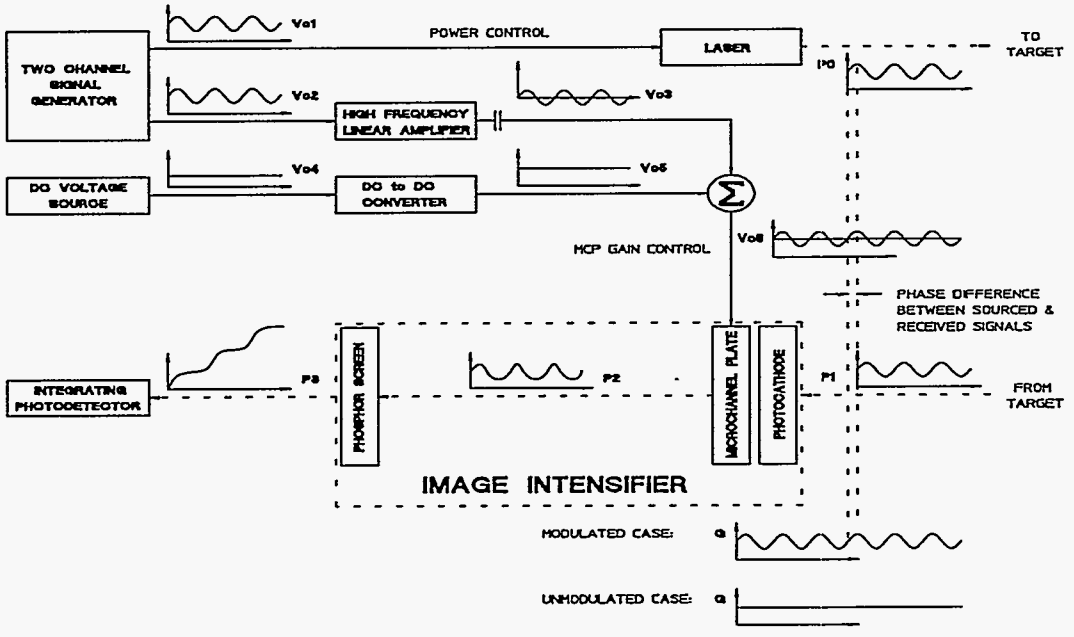

Fig. 1. Schematic diagram of the Scannerless Range Imager (SRI).

The variables shown in figure 1 are defined as follows:

V_{c1} is the modulated control voltage to the laser.
V_{c2} is the modulated gain control voltage to the MCP.
V_{c3} is the amplified AC portion of signal V_{c2}.
V_{c4} is the low level DC bias control voltage to the MCP.
V_{c5} is the high level DC bias control voltage to the MCP.
V_{c6} is the mixed ($V_{c3} + V_{c5}$) gain control voltage to the MCP.
P_0 is the modulated optical signal sourced by the laser.
P_1 is the received optical signal from the target reflection.
G is the electron gain produced in the image intensifier.
P_2 is the signal derived from mixing the signals P_1 and G.
P_3 is the signal derived from integrating P_2.

Using these variables the operation of the system can be described in greater detail. The transmitter output power is given by

$$P_0 = \overline{P}_0(1 + m_0 \sin(wt))$$

where $\overline{P}_0$ denotes the DC signal, m_0 denotes the depth of modulation, and w denotes the modulation frequency. Similarly the return signal is given by

$$P_1 = \overline{P}_1(1 + m_1 \sin(wt + \phi))$$

such that ϕ represents the relative phase delay between the returning and reference MCP gain signals corresponding with the distance traveled to and from an object in a given pixel. The phase delay is proportional to the relative range, r, as shown in the expression

$$r = \frac{c\phi}{2w}$$

where c represents the velocity of light. The gain of the MCP is modulated using the same radian frequency and phase as that of the transmitter thus providing a reference signal. The gain can be described as

$$G = \overline{G}(1 + m\sin(wt)).$$

The returned signal in each glass capillary of the MCP is simultaneously mixed such that the instantaneous output of any capillary is given by

$$A_c = \overline{P}_1(1 + m_1 \sin(wt + \phi))\overline{G}(1 + m\sin(wt)).$$

The mixed signals are then transmitted onto a CCD two dimensional array where integration takes place. If the integration time is an integer number of periods corresponding to the radian frequency w, the output of each pixel can be described as

$$A_p = \overline{P}_1\overline{G}(1 + \tfrac{1}{2} m_1 m \cos(\phi))nT$$

whereby nT denotes an integer number of periods. In order to extract pure range information, the same procedure is repeated with a nonmodulated gain

$$G = \overline{G}.$$

In this case, each individual capillary and pixel output are given by

$$B_c = \overline{P}_1(1 + m_1 \sin(wt + \phi))\overline{G}$$

$$B_p = \overline{P}_1\overline{G}nT$$

respectively. Thus, we can extract pure range information by dividing the two images collected with different intensifier gains on a pixel by pixel basis to get

$$C_p = 1 + \tfrac{1}{2} m_1 m \cos(\phi).$$

2. TEST DATA

The simple, rugged, and compact field system shown in figure 2 was built at Sandia to demonstrate proof of concept for the SRI technology. The principle used to extract range information does not require an optically coherent light

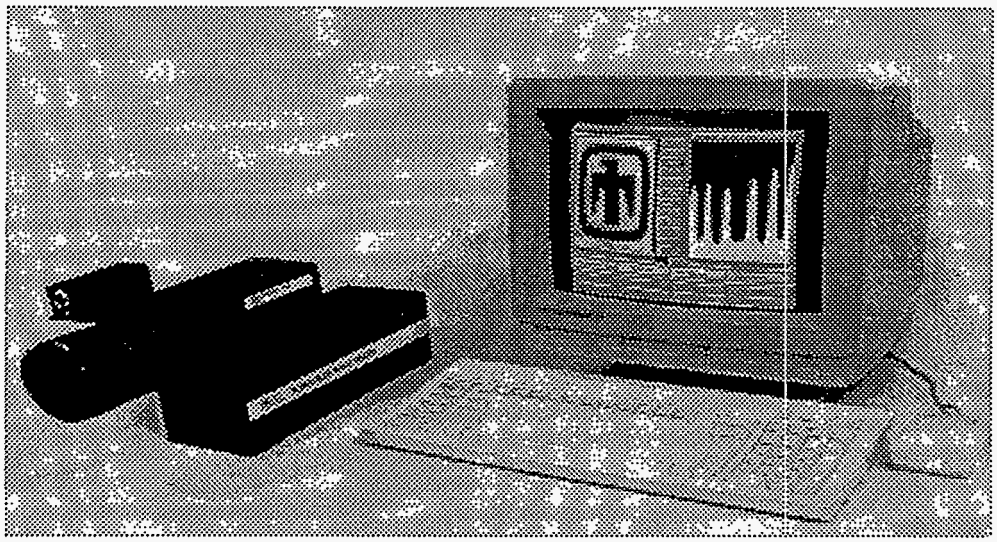

Fig. 2. SRI field unit.

source, thus various light sources including an array of light emitting diodes (LEDs) have been used to illuminate the image scene. Figure 3 is a photograph of a scooter at approximately 63 feet and a man at approximately 53 feet distance from the SRI system. Figures 4 and 5 show the SRI intensity and processed range 256 x 256 images of the scene shown in figure 3. The SRI images were collected using a red LED array transmitter modulated at 5 Mhz and collected at night in order to yield a higher SNR.

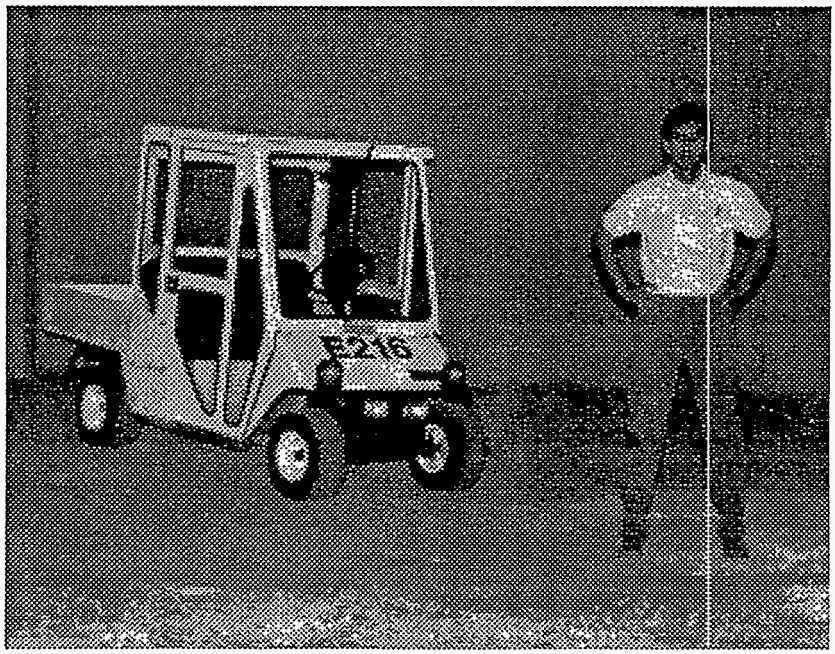

Fig. 3. Photograph of man and scooter.

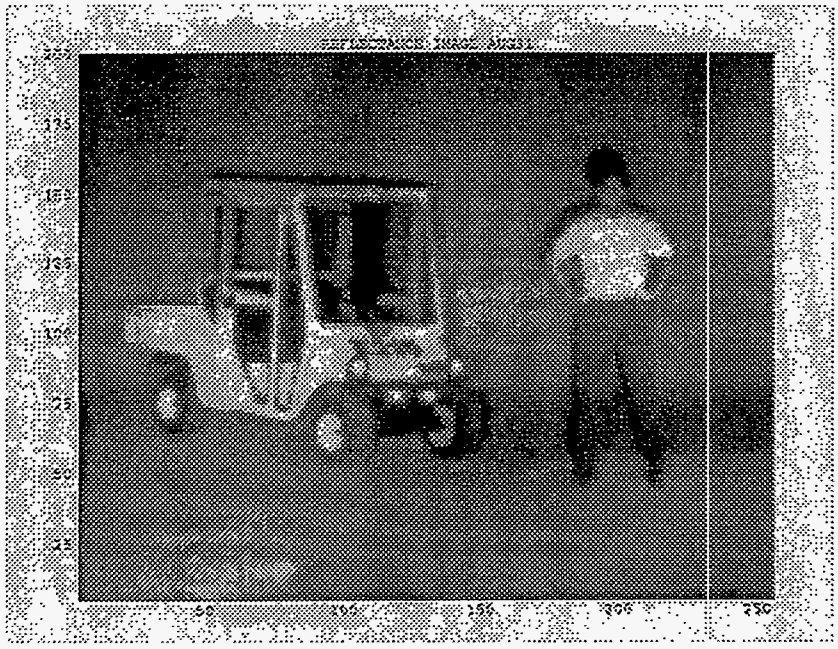

Fig. 4. SRI intensity image.

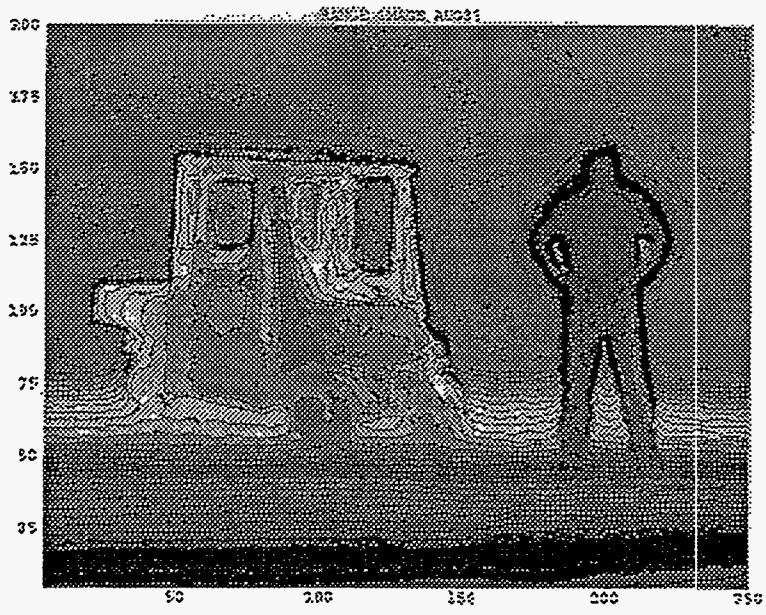

Fig. 5. SRI range image.

3. MOTIVATION FOR THE SQUARE WAVE

The SRI configuration illustrated above is an eye safe, inexpensive, and high frame rate system. However, in order to increase the range resolution, reach further distances, and compete with the sun which radiates approximately 1 $W/m^2/nm$ at 800 nm, the transmitter must emit more power. Laser diode arrays with up to 100 W of power are readily available off the shelf; however, these lasers present a couple of problems. They require high operating currents, typically 36 A for a 20 W continuous wave, laser diode array, and they have very low impedances, typically 0.02 Ω in series. The drivers required to operate these lasers in excess of 1 Mhz simply do not exist commercially. In an effort to design a driver

to incorporate a more powerful transmitter, it appeared more prudent to use a square wave rather than a sinusoidal wave. A square wave can be produced by simply turning the power on and off which is more energy efficient. Thus, a new algorithm to extract range information from a different waveform from the original SRI design was investigated.

4. SQUARE WAVE ALGORITHM

There is no inherent principle in Marion Scott's invention of the SRI which prescribes a sinusoidal wave. A square wave may be employed by driving the transmitter and MCP gain with a 50% duty cycle pulse. Using the same variables described above, figure 6 illustrates the square wave mode of operation.

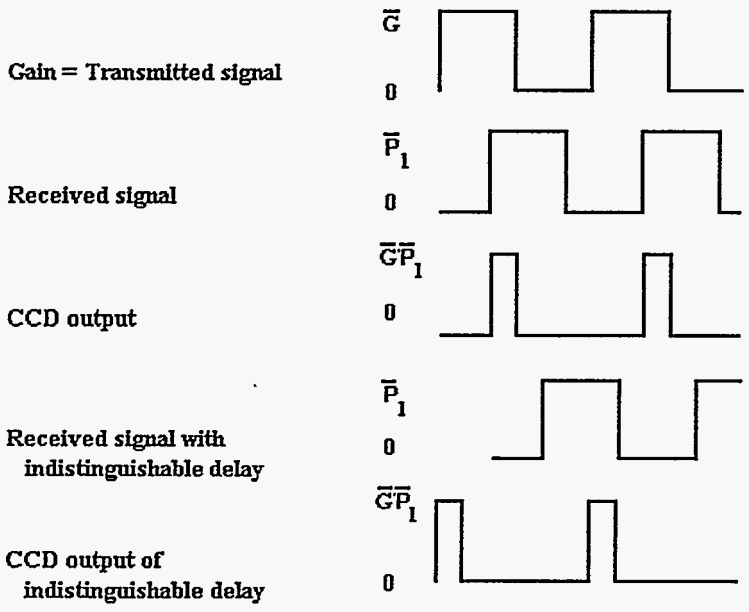

Fig. 6. Square wave mode of operation.

The CCD output per pixel is given by

$$P_3 = \int_t^{t+nT} \overline{GP_1} d\tau = n \int_t^{T/2} \overline{GP_1} d\tau = n\overline{GP_1}(T/2 - t),$$

and the time delay t is related to the range

$$R = \frac{ct}{2}.$$

Note in figure 6 that the CCD output for each time delay is not unique. Each time delay in the first half of the period has a corresponding, undistinguishable time delay in the second half of the period which is the mirror image of the first waveform about 3T/4 in the reference gain waveform. The undistinguishable corresponding CCD output with $t > T/2$ may be expressed as

$$P_3 = n \int_0^{t-T/2} \overline{GP_1} d\tau = n\overline{GP_1}(t - T/2).$$

The two delays may be distinguished by obtaining another measurement with the gain waveform shifted by T/4 as is done to obtain unambiguous 0 to 2π phase delays in the sinusoidal mode of operation. Figure 7 illustrates how the CCD which was previously undifferentiated can now be distinguished.

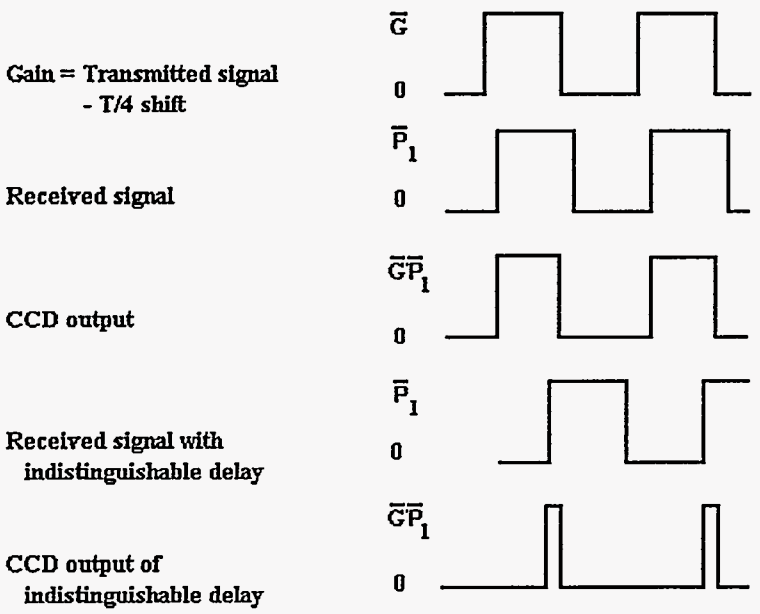

Fig. 7. Shifting to extract unambiguous range data.

With the gain shifted by T/4, the CCD output becomes

$$P_3 = n \int_{t}^{3T/4} \overline{GP_1} d\tau = n\overline{GP_1}(3T/4 - t)$$

for T/4 < t <3T/4, or

$$P_3 = n \int_{T/4}^{t+T/2} \overline{GP_1} d\tau = n\overline{GP_1}(t + T/4)$$

for t < T/4, or

$$P_3 = n \int_{T/4}^{t-T/2} \overline{GP_1} d\tau = n\overline{GP_1}(t - 3T/4)$$

for t > 3T/4. Let A represent the measured pixel value of P_3 when the reference gain waveform is not shifted relative to the transmitter signal, and let B represent the value of P_3 with the T/4 shifted gain. The following observations may be easily visualized.

t	A	B	A/B
T/2	0		
3T/4		0	
0			2
T/4			1/2

Other time delays between 0 to T may be calculated using the respective ratios for the time intervals derived above.

t	A/B	A/B Range
0 - T/4	$\frac{T/2 - t}{t + T/4}$	$\frac{1}{2} < \frac{A}{B} < 2$
T/4 - T/2	$\frac{T/2 - t}{3T/4 - t}$	$0 < \frac{A}{B} < \frac{1}{2}$
T/2 - 3T/4	$\frac{t - T/2}{3T/4 - t}$	$0 < \frac{A}{B} < \infty$
3T/4 - T	$\frac{t - T/2}{t - 3T/4}$	$2 < \frac{A}{B} < \infty$

Note that the ratio A/B contains pure range information as $nG\overline{P_1}$ cancels on a pixel by pixel basis. This table shows that all time delays have not yet been differentiated. By shifting the reference waveform again by another T/4, the following ratios may be calculated as illustrated above. C represents the pixel value of P_3 with the relative T/2 shift in the gain waveform.

t	B/C	B/C Range
0 - T/4	$\frac{t + T/4}{t}$	$2 < \frac{B}{C} < \infty$
T/4 - T/2	$\frac{3T/4 - t}{t}$	$\frac{1}{2} < \frac{B}{C} < 2$
T/2 - 3T/4	$\frac{3T/4 - t}{T - t}$	$0 < \frac{B}{C} < \frac{1}{2}$
3T/4 - T	$\frac{t - 3T/4}{T - t}$	$0 < \frac{B}{C} < \infty$

Again, all time delays have not been differentiated. A fourth frame with a 3T/4 shift in the reference waveform is required to differentiate all time delays. D represents this fourth measurement.

t	C/D	C/D Range
0 - T/4	$\frac{t}{T/4 - t}$	$0 < \frac{C}{D} < \infty$
T/4 - T/2	$\frac{t}{t - T/4}$	$2 < \frac{C}{D} < \infty$
T/2 - 3T/4	$\frac{T - t}{t - T/4}$	$\frac{1}{2} < \frac{C}{D} < 2$
3T/4 - T	$\frac{T - t}{5T/4 - t}$	$0 < \frac{C}{D} < \frac{1}{2}$

Now all of the time intervals have been decisively isolated, and the most robust corresponding formula may be applied to obtain the time delay. Thus, with only one more image frame than required in the sinusoidal modulation mode of operation proposed in the original invention, unambiguous 0 to T range data can be extracted from a square wave.

5. ACKNOWLEDGMENTS

This work was supported by the United States Department of Energy under Contract DE-AC04-94AL85000.

6. REFERENCES

1. John T. Sackos, "Derivation of New Equations," *Sandia National Laboratories Internal Technical Memorandum*, August 1992.

DISCLAIMER